GEORGETOWN SCIENTIFIC RESEARCH JOURNAL

Volume Four
Edition One
Spring 2024

Intradermal Injection of Bleomycin Shows Preliminary Evidence of Dermal Fibrosis in a Mouse Model

Tharun Potluri, Cameron S. D'Orio, BS, Lauren T. Moffatt, PhD, Jeffrey W. Shupp, MD, Bonnie C. Carney, PhD

Intradermal Injection of Bleomycin Shows Preliminary Evidence of Dermal Fibrosis in a Mouse Model

Tharun Potluri[1,2], Cameron S. D'Orio, BS[2], Lauren T. Moffatt, PhD[2,3], Jeffrey W. Shupp, MD[2,3,4,5], Bonnie C. Carney, PhD[2,3]

[1] Department of Human Science, School of Health, Georgetown University, Washington DC, USA
[2] Firefighters' Burn and Surgical Research Laboratory, MedStar Health Research Institute, Washington DC, USA
[3] Departments of Surgery and Biochemistry and Molecular & Cellular Biology, Georgetown University School of Medicine, Washington DC, USA
[4] Department of Plastic Surgery, Georgetown University School of Medicine, Washington DC, USA
[5] Department of Surgery, The Burn Center, MedStar Washington Hospital Center, Washington DC, USA
Email: tp600@georgetown.edu
https://doi.org/10.48091/gsr.v3i2.70

Abstract

Burn wounds can result in the development of hypertrophic scar (HTS). A problematic characteristic of HTS is dyschromia, which is often distressing to patients and has been shown to impact quality of life. There are currently no viable, non-surgical treatment methods for dyschromia, and the mechanisms of its etiology are not well understood. We aimed to test if the fibrotic microenvironment of the dermis plays a contributing role in the development of epidermal dyschromia. To do this, we focused on reproducing a previously published model of bleomycin-induced dermal fibrosis to add to the replicability of previous findings and establish a reliable model to serve as a basis for understanding post-burn dyschromia development. By treating C57BL/6 mice with intradermal injections of three varying doses of bleomycin for two weeks and conducting histological and molecular analyses of collected data, we were able to assess the adequacy of dermal fibrosis development. Collected data showed evidence of hair follicle obliteration, dermal thickening, and other characteristics of fibrotic architecture within all three bleomycin-treated groups, bust mostly profoundly in the high-dose group. However, qRT-PCR data did not reveal any significant trends in differential expression of genes of interest. In future work, additional qRT-PCR analysis, immunofluorescence visualization, and other molecular assays should be conducted to obtain further molecular confirmation of bleomycin-induced dermal fibrosis before we can attempt to understand the mechanistic relationship between dermal fibrosis and epidermal dyschromia.

Keywords: hypertrophic scar, dyschromia, fibrosis, bleomycin

1. Introduction

Recent advances in the management and treatment of burn-related injuries have led to a significant decrease in mortality rates, especially for large total body surface area full-thickness burns.[1] With an increasing patient survival rate, attention is now being turned to managing the after-effects of burn injury. Burn wounds and other cutaneous trauma can result in the development of hypertrophic scar (HTS), among other physiological complications such as muscle wasting, contractures, infection, and more.[2] HTS is typically raised, thick, non-pliable, erythematous, pruritic, and painful.[3] Irregular inflammatory processes in the dermis contribute to

HTS pathophysiology. HTS forms as a result of excess collagen deposition and abnormal fibroblast proliferation. The abnormal functioning of these fibroblasts results in excess amounts of extracellular matrix components that cause elevated and stiff skin characteristic of HTS.[4] The bulk of HTS tissue is composed of the dermis layer which is primarily made up of type 1 collagen, fibroblasts, and endothelial cells.[5] A number of proteins, such as collagen 1 alpha 1 (COL1A1), COL1A3, transforming growth factor beta-1 (TGFB1), and galectin-1 (LGALS1), have been shown to be differentially overexpressed in fibrotic skin characteristic of HTS.[6] Additionally, HTS typically has thickened dermis and epidermis layers and a change in collagen architecture that causes the increased skin stiffness.

In addition to the physical impacts of post-burn HTS development, patients with HTS frequently suffer from the psychosocial impacts of altered appearance and restricted range of motion that often results due to HTS.[7] Almost all HTSs display dyschromia, which appears as hypo- or hyperpigmentation of the skin. More severe scars with extreme dermal pathology (increased thickness, hyper-vasculature, hyper-cellularity, non-pliability, contracture) often exhibit the most profound dyschromia. Dyschromic HTS, which develops pervasively amongst patients with skin of color, is often distressing to patients and has been shown to impact quality of life metrics such as stigmatization, sexual health, and physiological health.[8-12] While some therapies have led to modest improvements in HTS symptoms for some patients, HTS and its psychosocial impact continues to be challenging to treat. Finding viable, non-surgical treatment methods for dyschromia could significantly improve the quality of life for patients with HTS.

Before testing treatment methods, however, the mechanistic processes behind dyschromia must first be understood. There is currently a large gap in knowledge as to how post-burn dyschromia actually develops, which is underscored by the paucity of literature surrounding the topic. One hypothesis is that dyschromia develops due to abnormalities in the paracrine signaling between melanocytes and surrounding cell types.[13] In fibrotic skin, fibroblasts are in an altered state of inflammation that could influence melanocyte function, which can be quantifiably assessed by melanin index.[14] However, it is also possible that fibroblasts do not contribute to dyschromia at all, and that keratinocytes play a more significant role. Understanding the cellular abnormalities that cause dyschromia is a crucial first step in the effort to develop treatments for dyschromic HTS. Thus, a reliable and repeatable model for HTS must be established by which dyschromia can be studied.

Not only does skin fibrosis develop as a result of burn wounds (HTS), but it can also occur due to various disease processes. A common disease that results in skin fibrosis is systemic sclerosis.[15] Patients with this disease have thickened skin that looks similar to burn scars and often exhibits dyschromia classified as "salt-and-pepper" skin.[16] An approach that has previously been taken by other researchers is to study non-HTS dermal fibrosis by synthetically inducing fibrosis with a commonly used antineoplastic drug called bleomycin. A study conducted by Błyszczuk et al. showed the efficacy of bleomycin-induced dermal fibrosis in a mouse model through regular injections of bleomycin.[14]

This study aims to reproduce this published model of bleomycin-induced dermal fibrosis in an effort to establish the utility of this model for the study of HTS dyschromia.

2. Methods

In this study, two groups of mice were tested. Following the completion of Group 1 mice, data was collected and analyzed before starting the next group. Using lessons learned from the Group 1 mice, Group 2 mice had a refined experimental procedure in an effort to produce more conclusive results.

All animal work was approved by the MedStar Health Research Institute's Institutional Animal Care and Use Committee. Facility standard operating procedures under an animal care and use program accredited by the Association for Assessment and Accreditation of Laboratory Animal Care International were strictly followed

for handling and care of all the animals used in this study.

2.1 Group Selection, Anesthesia, and Pretreatment Procedures

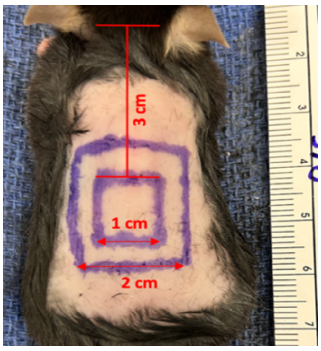

Figure 1. Dorsal demarcation of the injection site. The 1cm x 1cm demarcated square is where all injections occurred. This square was drawn 3cm below the midline of the ears on each mouse for standardization. A 2cm x 2cm square was demarcated as a "buffer zone" to account for spreading of bleomycin or saline control outside of the 1cm x 1cm injection square.

Female C57-BL/6 mice (22-45±6.59g) were used in Group 1 (n=3 in control, high-dose, mid-dose, n=4 in low-dose groups). In Group 2, female C57-BL/6 mice (19-23±1.11g) were used (n=5 in control, n=4 in high-dose, mid-dose, low-dose groups). Anesthesia was induced by placing the mice into a box with 3-5% isoflurane. Once a plane of anesthesia was established by confirming absence of corneal and pedal reflexes, anesthesia was continued via nose cone administration of 1-4% isoflurane. Ophthalmic ointment was used in cases of prolonged anesthesia. Thermoregulation was achieved with a warming blanket during anesthesia procedures. During the pre-injury timepoint, the dorsum of the mouse was shaved using standard veterinary clippers and depilated using a commercial agent for 90 seconds with massage of the agent into the skin with a cotton swab (Nair, Church & Dwight Co., Ewing, NJ). In Group 1 mice, a 1 cm x 1 cm square was demarcated 3 cm below the midline of the ears using a surgical marker (Figure 1). In Group 2 mice, a 2 cm x 2 cm square was demarcated around the 1 cm x 1 cm square (Figure 1). In addition to baseline weights, non-invasive skin probe measurements (elasticity, trans-epidermal water loss, erythema, melanin) (Delfin Technologies, Kuopio, Finland) were also taken within the demarcated area. Mice were placed on their sides with their hind legs facing the same direction during probe measurements to reduce the pressure of the probe on the spine.

2.2 Bleomycin Injection and Monitoring

Lyophilized bleomycin sulphate (Sigma-Aldrich, St. Louis, MO) was dissolved in normal saline. 100 µl of bleomycin or saline control was injected on days 1, 2, 4, 5, 8, 9, 11, and 12 for Group 1, and days 1, 2, 5, 6, 8, 9, 12, and 13 for Group 2. Injections were administered intradermally into the 1 cm x 1 cm square at different positions on different days (Figure 2). On day 1, injections were performed at position 1, on day 2 at position 2, continuing in this fashion throughout the time course. After position 5, injections were further continued cyclically starting again at position 1. This injection pattern, which was based off of previously published literature, ensured that the bleomycin was distributed equally across the entire demarcated treatment zone.[14]

Three different dosages of bleomycin were tested in each group. In Group 1 mice, low-dose (0.5 U/mL), mid-dose (1.0 U/mL), and high-dose (5 U/mL) bleomycin was used. In Group 2, the high-dose concentration was adjusted to 2.5 U/mL. After injection, mice were removed from anesthesia and monitored until ambulatory. Non-invasive skin probe measurements of the treated zone and normal skin were taken periodically throughout the study and were collected in triplicate for each probe. Animal checks were conducted twice a day at minimum and mice weights were obtained each day. Mice with weight loss of 5% compared to their initial weight or with obvious signs of distress were given a 1 mL intraperitoneal injection of lactated ringers daily in addition to DietGel dietary supplements (ClearH2O, Westbrook, ME). In Group 2 mice, all mice were given DietGels on day 1

prophylactically. The mice were never subjected to more than two days of back-to-back isoflurane anesthesia to prevent a negative reaction to cumulative anesthesia.

2.3 Terminal Timepoint

On day 15, all mice were placed under anesthesia and euthanized via exsanguination and cervical dislocation. Terminal weights and non-invasive probe measurements were obtained prior to euthanasia. Treated zone skin and normal skin were collected and preserved in Allprotect Tissue Reagent (Qiagen, Germantown, MD) and 10% neutral buffered formalin (NBF). Blood was collected and placed in RNAprotect tubes (Qiagen, Germantown, MD) and K2EDTA tubes, and was spun down to isolate plasma. Lungs were dissected and preserved in Allprotect Tissue Reagent (Qiagen, Germantown, MD) and NBF.

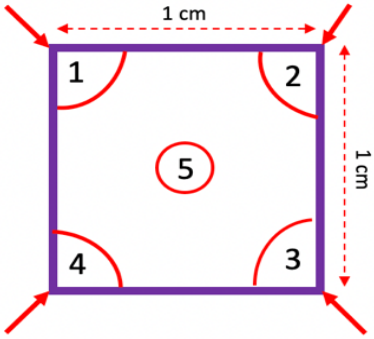

Figure 2. Injection pattern for intradermal injection of bleomycin or saline control. Injections were administered from positions 1 to 5 throughout the time course. After position 5, injections were further continued cyclically starting again at position 1.

2.4 *Histological Analysis*

Formalin-fixed skin and lung samples collected at the terminal timepoint were paraffin embedded, sectioned at 4 μm thickness onto slides, and stained with hematoxylin and eosin (H&E) as previously described.[17] Tile images were taken at 10X magnification to assess dermal architecture, dermal cellularity, and dermal and epidermal thickness using an Axio imager M2 microscope with motorized stage (Carl Zeiss Inc., Oberkochen, Germany) and an Axiocam 208 color camera. Zen blue software was used to export images (Carl Zeiss Inc., Oberkochen, Germany). ImageJ software was used to quantify dermal and epidermal thickness and 10 replicates were taken at different positions across the biopsy for each sample.

2.5 Confirmatory qRT-PCR Analysis

RNA from collected skin biopsies was isolated and purified for molecular assays using an automated protocol for the RNeasy fibrous tissue mini kit (Qiagen, Germantown, MD) with the Qiacube. RNA quality and quantity determined by spectro-photometry (Nandrop2000, ThermoFisher, Waltham, MA) and all samples were diluted to 1 ng/uL prior to running. Confirmatory qRT-PCR was conducted using a one-step reverse transcription and SYBR green kit (BioRad Laboratories Inc., Hercules, CA) to measure differential expression of COL1A1, COL1A3, TGFB1, and LGALS1 as previously described.[17] Glyceraldehyde 3-phosphate dehydrogenase (GAPDH) and ribosomal protein L13A (RPL13A) were used as housekeeping genes. Fold changed was assessed using ΔΔCt analysis.

2.6 Statistics

For non-invasive probe measurements and PCR data, a two-way ANOVA with multiple comparisons was run to compare differences across treatment groups and time points. Data was also analyzed as fold change at various time points to compare treatment to control at similar time points, or as fold change over time compared to the day of treatment initiation. For all analyses, $p<0.05$ was considered statistically significant. For qRT-PCR, fold change > or < 2 was established as the significance threshold. Outliers were excluded using Grubb's outlier test. GraphPad Prism 10 was used for data visualization.

3. Results

3.1 Bleomycin Treatment Resulted in Decreased Skin Elasticity

The high-dose bleomycin group showed a significant decrease in skin elasticity at the

terminal timepoint (day 15) compared to baseline measurements (day 1-4), indicating decreased skin pliability (58±22.9 vs 135.8±57.9 N/m) (Figure 3A). The low-dose group showed a similar decrease in skin elasticity over time (50.1±17.9 vs 91.1±34.1 N/m). However, there was no significant difference in skin elasticity over time in the mid-dose and control groups.

3.2 Melanin Index Increased Throughout the Duration of the Study in All Groups

Non-invasive probe data showed a 4-fold increase in melanin at the terminal timepoint (day 15) compared to baseline measurements (day 1-4) for the control group (628.7±42.4 vs 882.9±81.8) (Figure 3B). Similar trends were present for the low-dose group (648.4±60.6 vs 850.2±56.5) and mid-dose group (658.2±116.5 vs 867.2±52.6). The high-dose group did not show any significant difference in melanin index (746.6±132 vs 806.9±108.7).

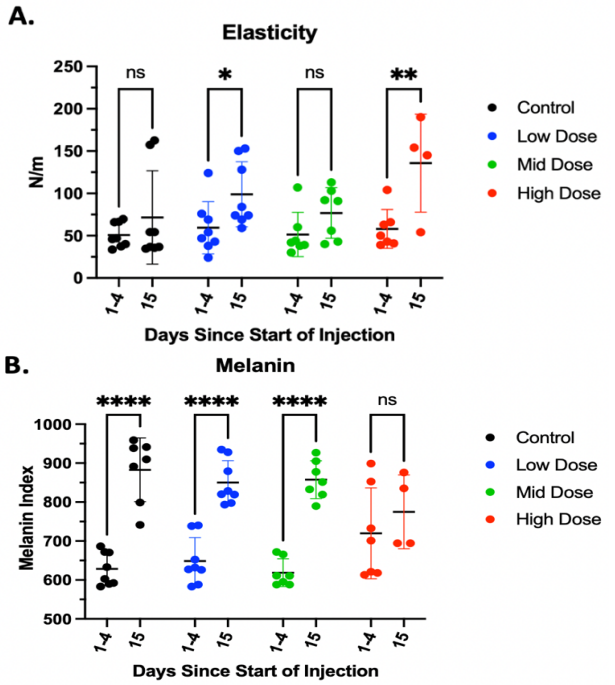

Figure 3. Elasticity and melanin measurements using non-invasive skin probes. (A) In the low-dose and high-dose groups, there was a significant increase in stiffness between days 1-4 and day 15 ($P < 0.05$). (B) Control, low-dose, and mid-dose groups showed significant increase in melanin index between days 1-4 and day 15. Values presented as mean ± SEM.

3.3 Histological Analysis Showed Changes to Dermal Architecture

Analysis of H&E-stained biopsies of the normal and treated zone in high-dose mice showed areas of dermal and epidermal thickening, hair follicle obliteration, and evidence of fibrotic architecture (Figure 4A). Mid- and low-dose mice showed similar dermal thickening, however changes to epidermal thickness and hair follicle architecture were less prominent than in the high dose group. Control mice treated zone skin appeared the same as normal skin, as expected.

Quantitative assessment of epidermal thickness (Figure 4B) and dermal thickness (Figure 4C) confirmed thickening of the epidermis (14.1±0.19 vs 38.8±4.83 μm) and dermis (104.7±11.1 vs 231±52.5 μm) in treated zone skin compared to normal skin for high-dose mice, however this difference did not reach significance ($p > 0.05$). Control, low-dose, and mid-dose skin not show any significant difference in epidermal or dermal thickness in the treated zone skin compared to normal skin.

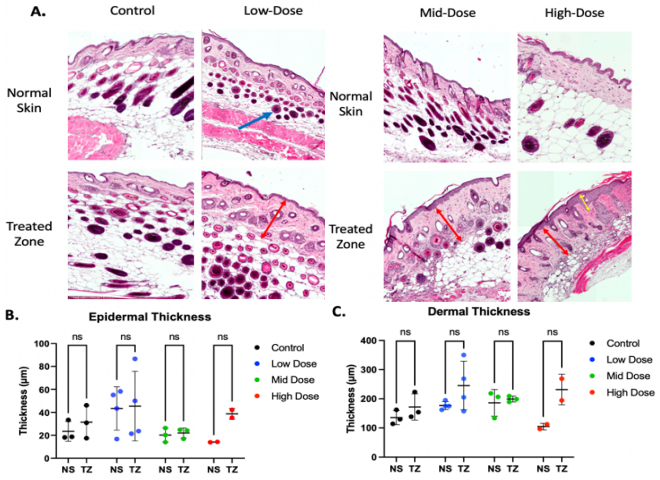

Figure 4. Effects of bleomycin treatment on dermal and epidermal architecture in a mouse model. (A) Biopsies of normal skin and treatment zone skin taken at the terminal timepoint were sectioned and H&E stained to be assessed for dermal thickness (red arrows), epidermal thickness (yellow arrow), hair follicle presence (blue arrow),

and other changes to dermal architecture. Quantitative measurements of (B) epidermal and (C) dermal thickness analyzed from H&E stained images. Values presented as mean ± SEM.

3.4 PCR Analysis Did Not Show Significant Differential Expression of Genes of Interest

Analysis of COL1A1, COL3A1, and TGFB1 qRT-PCR data between the normal skin and treated zone skin for each group did not show any significant differential expression (Figure 5A-C). Though there was an increase in expression of LGALS1 in the treated zone skin compared to normal skin in the low-dose, mid-dose, and high-dose mice, none of the comparisons reached significance (Figure 5D).

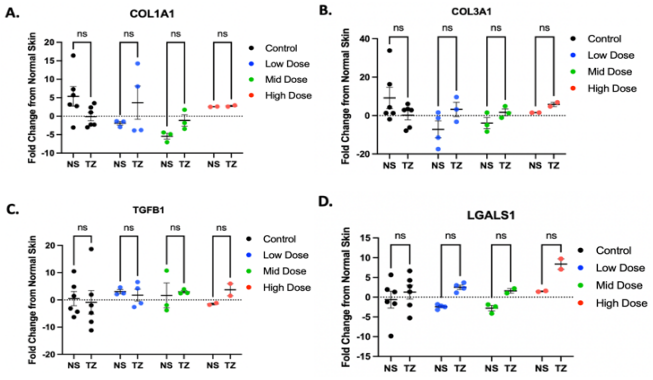

Figure 5. COL1A1 (A), COL3A1 (B), TGFB1 (C), and LGALS1 (D) expression in normal skin compared to treated zone skin for each group. RNA was isolated and purified from skin biopsies for confirmatory qRT-PCR analysis. Fold change was assessed using ΔΔCt analysis. $P < 0.05$ is considered statistically significant.

3.5 Bleomycin Treatment Resulted in Areas of Hair Loss Within the Treated Zone

Images taken at the terminal timepoint for each mouse revealed a trend of hair loss within the demarcated treated zone for the high-dose mice (Figure 6). A similar pattern of hair loss was also present in the mid- and low-dose groups, though not as prominent and widespread. Control mice did not show any evidence of hair loss within the treated zone.

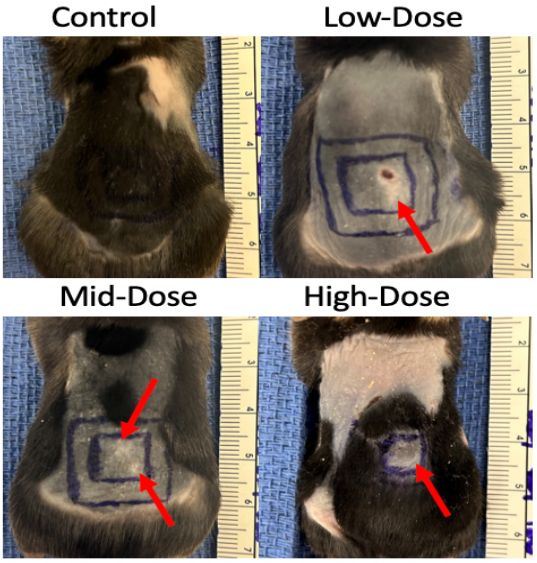

Figure 6. Representative images of the dorsal surface of high-dose, mid-dose, low-dose, and control mice at the terminal timepoint. Red arrows indicate areas of hair loss within the demarcated treated zone.

3.6 High-Dose Bleomycin Negatively Affects Mice Weights

All mice used in Groups 1 and 2 were weighed daily throughout the duration of the study. Group 1 high-dose mice lost a large amount of weight throughout the study duration, ending with a percent difference of -23.6% at the terminal timepoint compared to baseline measurements (Figure 7A). Group 1 control mice also dropped weight, though not as severely (-13.4%) at the terminal timepoint). Low-and mid-dose mice weights stayed relatively consistent. Group 2 control, low-, and mid-dose mice weights stayed relatively consistent, however high-dose mice lost a large amount of weight (-7.8% at the terminal timepoint) (Figure 7B).

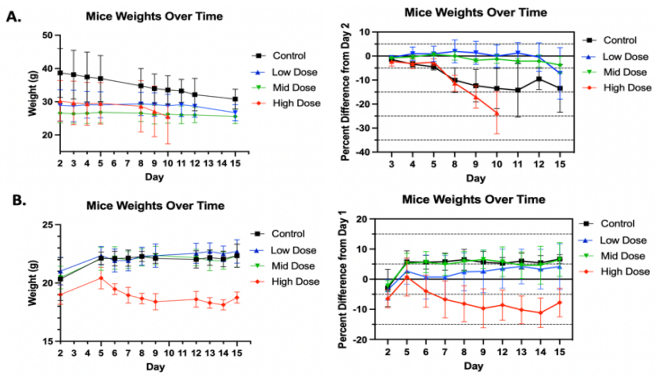

Figure 7. Mice weights for each group throughout the study duration. (A) Group 1 mice weights. (B) Group 2 mice weights. Mice weights were obtained each day. Percent difference calculations were obtained by comparing to initial mice weights on day 1. Mice with weight loss of 5% compared to their initial weight or with obvious signs of distress were given a 1 mL intraperitoneal injection of lactated ringers daily in addition to DietGel dietary supplements. All Group 2 mice were given DietGels on day 1 prophylactically. Values presented as mean ± SEM.

4. Discussion

This study aimed to confirm the experimental methods of a previously proven model of bleomycin-induced dermal fibrosis in mice within our laboratory. The eventual goal of being able to synthetically induce dermal fibrosis is to ascertain if there is a causal relationship between dermal fibrosis and epidermal dyschromia. Following regular injections of three different bleomycin doses and saline control into the dorsal skin of C57-BL/6 mice, data from non-invasive skin probes, histological analysis, and qRT-PCR analysis were used to determine if bleomycin injection induced dermal fibrosis.

One of the more promising markers of skin fibrosis is known to be skin elasticity.[17] Elasticity measurements were collected by non-invasive skin probes throughout the duration of this study. Analysis of probe data showed a significant decrease in skin elasticity at the terminal timepoint compared to baseline measurements for high-dose and low-dose groups, suggesting an increased skin thickness characteristic of dermal fibrosis. Interestingly, the mid-dose group did not show any significant difference in elasticity. One explanation for this finding is that the mid-dose mice had an increased presence of self-mutilated skin (caused by stress, irritation, etc.) which could have affected elasticity measurements. Imaging of H&E-stained skin biopsies showed clear epidermal and dermal thickening indicative of fibrotic architecture in the high-dose, mid-dose, and low-dose mice, though less prominent in the latter two groups. Differences in treated zone versus normal skin thickness might not have reached significance due to improper collection of normal skin. Normal skin was collected directly outside of the 2cm x 2cm demarcated outer square. As a result, some of the bleomycin could have spread outside of the demarcated injection site and caused changes to the skin outside of the treated zone, potentially influencing skin thickness measurements. Collection of normal skin further away from the treated zone should be performed in future studies to account for this problem. High-dose skin biopsies showed clear obliteration of hair follicles in the dermis caused by the bleomycin treatment, providing further evidence supporting the efficacy of the drug. Hair loss within the treated zone could also be seen on the images taken of the dorsal surface of the bleomycin-treated groups.

Collected qRT-PCR data did not show any statistically significant differences in differential expression in the treated zone skin compared to the normal skin for genes of interest. A potential explanation for this lack of significance is that the bleomycin destroyed tissue architecture and cellular function to such an extent that cells were unable to undergo gene transcription. However, an increase in expression of LGALS1 in the low-, mid-, and high-dose mice was observed. Increased presence of LGALS1 provided some molecular evidence of fibrotic development within the treated zone, though perhaps other genes should be assessed for further confirmation of fibrosis.[18] In future work, immunofluorescence visualization of α-SMA-positive myofibroblasts should be conducted and assessed for further molecular confirmation.[19]

In addition to affecting the dermal and epidermal histoarchitecture of the mice, bleomycin also seemed to have systemic effects on the mice as observed by changes in their weights. Group 1 high-dose mice were injected with a 5 U/mL concentration of bleomycin, whereas Group 2 high-dose mice were injected with a 2.5 U/mL concentration. These dosages were arbitrarily chosen and were not based on previously proven models as the literature did not report specific dosage values for study replication. This problem was the main issue we faced when attempting to

replicate the previously proven model. The dosage of bleomycin was adjusted for Group 2 due to the significant weight loss that was observed in Group 1 mice. Group 1 high-dose mice lost more weight overall than Group 2 high-dose mice. However, in addition to receiving a lower dosage of bleomycin, Group 2 mice were also prophylactically given Dietgels at the beginning of the study in an effort to mitigate weight loss. These two changes to the study protocol clearly helped reduce the amount of weight the mice lost throughout the study. In future work, RNA from lung biopsies and blood samples should be isolated and analyzed via qRT-PCR to look for evidence of systemic impacts of bleomycin.

The C57-BL/6 mice used in this study lack melanocytes within the skin, however melanin index significantly increased in control, low-dose, and mid-dose mice throughout the study duration. An explanation for this finding is that hair regrowth influenced melanin measurements in the mice. This would also explain why the high-dose mice did not show a significant difference in melanin index because the high-dose mice experienced hair loss as a result of bleomycin, limiting the extent to which melanin measurements were falsely influenced. The application of Nair during depilation seemed to induce hair follicle neogenesis or induction of the hair cycling pathway, which further affected melanin measurements. Further investigation needs to be conducted on the influence on depilating agents on hair follicle neogenesis and induction of cycling to better understand how to account for this problem in future work. Additionally, melanin content can be assessed via Fontana Masson staining techniques instead of non-invasive probes measurements for more accurate results. Fontana-Masson staining allows for visual-ization of melanin within the epidermis of the skin.

Elasticity measurements and H&E-stained skin biopsies showed evidence of bleomycin-induced dermal fibrosis in all three drug treatment groups, but most profoundly in the high-dose group. However, additional qRT-PCR analysis, immuno-fluorescence visualization, and other molecular assays should be conducted to obtain significant molecular confirmation of fibrosis. Further evidence is needed to confirm the efficacy of bleomycin-induced dermal fibrosis before attempting to understand the mechanistic relationship between dermal fibrosis and epidermal dyschromia.

References

1. Aarabi, S., Longaker, M.T., & Gurtner, G.C. (2007). Hypertrophic scar formation following burns and trauma: new approaches to treatment. *PLoS Med. 4*(9), 1464-70. https://doi.org/10.1371/journal.pmed.0040234
2. Finnerty, C.C., Jeschke, M.G., Branski, L.K., Barret, J.P., Dziewulski, P., & Herndon, D.N. 2016. Hypertrophic scarring: the greatest unmet challenge after burn injury. *Lancet. 388*(10052), 1427-36. https://doi.org/10.1016/S0140-6736(16)31406-4
3. Chiang, R.S., Borovikova, A.A., King, K., Banyard, D.A., Lalezari, S., Toranto, J.D., Paydar, K.Z., Wirth, G.A., Evans, G.R., & Widgerow, A.D. (2016). Current concepts related to hypertrophic scarring in burn injuries. *Wound Repair Regen. 24*(3), 466-77. https://doi.org/10.1111/wrr.12432
4. Van der Veer, W.M., Bloemen, M.C., Ulrich, M.M., Molema, G., van Zuijlen, P.P., Middelkoop, E., & Niessen, F.B,. (2009). Potential cellular and molecular causes of hypertrophic scar formation. *Burns. 35*(1), 15-29. https://doi.org/10.1016/j.burns.2008.06.020
5. Huang, C., Murphy, G.F., Akaishi, S., & Ogawa, R. (2013). Keloids and Hypertrophic Scars: Update and Future Directions. Plastic and Reconstructive Surfery. *1*(4), e25. https://doi.org/10.1097/GOX.0b013e31829c4597
6. Limandjaja, G.C., van den Broek, L.J., Waaijman, T., van Veen, H.A., Everts, V., Monstrey, S., Scheper, R.J., Niessen, F.B., & Gibbs, S. (2020). Increased epidermal thickness and abnormal epidermal differentiation in keloid scars. *Dermatologic Surgery. 176(*1), 116-126. https://doi.org/10.1111/bjd.14844
7. Nițescu, C., Calotă, D.R., Stăncioiu, T.A., Marinescu, S.A., Florescu, I.P., & Lascăr, I.

(2012). Psychological impact of burn scars on quality of life in patients with extensive burns who received allotransplant. *Romanian Journal of Morphology & Embryology*. *53*(3), 577-83.
8. Zeitlin, R.E. (1997). Long-term psychosocial sequelae of paediatric burns. *Burns*. *23*(6), 467-472. https://doi.org/10.1016/s0305-4179(97)00045-4
9. Ross, E., Crijns, T.J., Ring, D., & Coopwood, B. (2021). Social factors and injury characteristics associated with the development of perceived injury stigma among burn survivors. *Burns*. *47*(3), 692-697. https://doi.org/10.1016/j.burns.2020.07.022
10. Stoddard, F.J. Jr., Ryan, C.M., & Schneider, J.C. (2014). Physical and psychiatric recovery from burns. *Surgical Clinics of North America*. *94*(4), 863-78. https://doi.org/10.1016/j.suc.2014.05.007
11. Taal, L., & Faber, A.W. (1998). Posttraumatic stress and maladjustment among adult burn survivors 1 to 2 years postburn. Part II: the interview data. *Burns*. *24*(5), 399-405. https://doi.org/10.1016/s0305-4179(98)00053-9
12. Wisely, J.A., Hoyle, E., Tarrier, N., & Edwards, J. (2007). Where to start? Attempting to meet the psychological needs of burned patients. *Burns*. 33(6), 736-46. https://doi.org/10.1016/j.burns.2006.10.379
13. Baugh, E.G., Anagu, O., & Kelly, K.M. (2022). Laser Treatment of Hypopigmentation in Scars: A Review. *Dermatologic Surgery*. *48*(2), 201-206. https://doi.org/10.1097/DSS.0000000000003330
14. Błyszczuk, P., Kozlova, A., Guo, Z., Kania, G., & Distler, O. (2019). Experimental Mouse Model of Bleomycin-Induced Skin Fibrosis. *Current Protocols in Immunology*. *126*(1), e88. https://doi.org/10.1002/cpim.88
15. Jawitz, J.C., Albert, M.K., Nigra, T.P., & Bunning, R.D. (1984). A new skin manifestation of progressive systemic sclerosis. *Journal of the American Academy of Dermatology*. *11*(2), 265. https://doi.org/10.1016/s0190-9622(84)70163-0
16. Sakamoto, T., Kaburaki, M., & Shimizu, T. (2021). Salt-and-pepper skin appearance and systemic sclerosis. *QJM. 114*(8), 599-600. https://doi.org/10.1093/qjmed/hcab070
17. Carney, B.C., Chen, J.H., Luker, J.N., Alkhalil, A., Jo, D.Y., Travis, T.E., Moffatt, L.T., Simbulan-Rosenthal, C.M., Rosenthal, D.S., & Shupp, J.W. (2019). Pigmentation Diathesis of Hypertrophic Scar: An Examination of Known Signaling Pathways to Elucidate the Molecular Pathophysiology of Injury-Related Dyschromia. *Journal of Burn Care & Research*. *40*(1), 58-71. https://doi.org/10.1093/jbcr/iry045
18. Kirkpatrick, L.D., Shupp, J.W., Smith, R.D., Alkhalil, A., Moffatt, L.T., & Carney, BC. (2021). Galectin-1 production is elevated in hypertrophic scar. *Wound Repair & Regeneration*. *29*(1), 117-128. https://doi.org/10.1111/wrr.12869
19. Tejiram, S., Zhang, J., Travis, T.E., Carney, B.C., Alkhalil, A., Moffatt, L.T., Johnson, L.S., & Shupp, J.W. (2016). Compression therapy affects collagen type balance in hypertrophic scar. *Journal of Surgical Research*. *201*(2), 299-305. https://doi.org/10.1016/j.jss.2015.10.040